Effect of Local Structure of $MnCl_2$-Filled PVDF Films on Their Optical, Electrical, Electron Spin Resonance, and Magnetic Properties

A. TAWANSI,[1] A. H. ORABY,[1] E. M. ABDELRAZEK,[1] M. I. AYAD,[2] M. ABDELAZIZ[1]

[1] Physics Department, Faculty of Science, Mansoura University, 35516, Egypt

[2] Chemistry Department, Faculty of Science, Shibinelkoam University, Egypt

Received 13 March 1997; accepted 21 July 1997

ABSTRACT: The filling level (W) dependence of the local structure of $MnCl_2$ through the PVDF matrix was explored. The presence of α- and β-PVDF crystalline phases were detected by X-ray diffraction, and it was confirmed by the infrared (IR) absorption spectra. A significant head-to-head content was implied by IR spectroscopy. Two filling, level-dependent optical energy gaps were found through the UV–VIS spectral investigation. An intrachain one-dimensional interpolaron hopping mechanism was assumed to proceed in the temperature range of 350–375 K. The calculated values of the charge carrier hopping distance were in the range of 6.5–9.7 nm. The temperature dependence of the direct current (dc) magnetic susceptibility exhibited a Curie–Weiss behavior. Positive values of the paramagnetic Curie temperature (θ_p) for W up to 14.5% indicated the presence of a ferromagnetic interaction, while negative θ_p obtained for higher W values suggested an antiferromagnetic interaction at lower temperature. The electron spin resonance (ESR) analysis revealed the existance of both isolated and aggregated Mn^{2+} ions within the PVDF matrix. © 1998 John Wiley & Sons, Inc. J Appl Polym Sci 70: 1437–1445, 1998

Key words: $MnCl_2$-filled PVDF; X-ray diffraction; optical; electric; electron spin resonance; magnetic properties

INTRODUCTION

Due to its strong piezoelectricity,[1] sensitive pyroelectricity,[2] nonlinear optical properties[3] applicability in infrared to visible conversion,[4] and microwave response,[5] PVDF, in its various crystalline forms and several of its copolymers,[6] has been extensively studied during the last three decades. Space charge and ferroelectric dipolar effects in these polymers have been already well explored.[7] Moreover, an increasing interest has been devoted to PVDF as an electric and/or magnetic field sensor.[8] For this application, PVDF was filled with transition metal halides (TMH).[9] However, the knowledge of the effect of the local structure of TMH on the physical properties of polymers is incomplete so far,[10] and some aspects deserve further studies.

Manganese is well known as a magnetoactive multivalent element. Thus, its halides can be used as fillers to modify the electric conduction, the optical absorption, and the magnetic properties of PVDF. On the other hand, $MnCl_2$ is considered as a good candidate for one- or two-dimensional phenomena.[11]

The present work is devoted to study the effect

Correspondence to: A. Tawansi.

Journal of Applied Polymer Science, Vol. 70, 1437–1445 (1998)
 CCC 0021-8995/98/081437-09

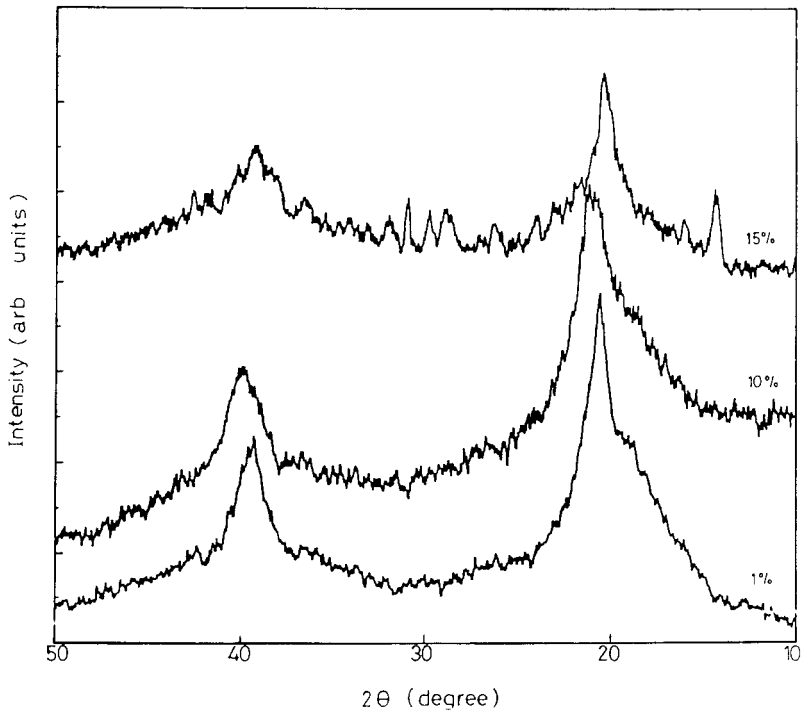

Figure 1 X-ray diffraction scans of various $MnCl_2$ filling levels for PVDF films.

of local structure of $MnCl_2$-filled PVDF films on their optical, electrical, electron spin resonance (ESR), and magnetic properties.

EXPERIMENTAL

The studied PVDF films were prepared by a casting method. PVDF powder (SOLEF 1008) was dissolved in dimethylformamide (DMF). $MnCl_2$ was also dissolved in DMF. The solution of $MnCl_2$ was added to the dissolved polymer with a suitable viscosity. The mixture was cast to a glass dish and kept in a dry atmosphere at 30°C for two weeks to insure removal of solvent traces. The thickness of the obtained films was of the range 0.1 to 0.5 mm. PVDF films of the following $MnCl_2$ mass fractions were prepared: 0, 0.001, 0.01, 0.1, 0.5, 1.0, 5.0, 10.0, 15.0, and 25%.

The X-ray diffraction (XRD) scans were obtained using a Seimens type F diffractometer with CuKα radiation and a LiF monochromator. An infrared (IR) spectrophotometer (Perkin–Elmer 883) was used for measuring the IR spectra in the wave number range of 200–4000 cm^{-1}. UV–IVS absorption spectra were measured in the wavelength region of 200–800 nm using a spectrometer (Perkin–Elmer UV–IVS). The ESR spectra were recorded on JEOL spectrophotometer (type JES–FE2XG) at frequency of 9.45 GHz, using DPPH as a calibrant. The magnetic susceptibility was measured using Faraday pendulum balance technique of an accuracy better than = 3%. Diamagnetic corrections were done.

RESULTS AND DISCUSSION

X-ray Diffraction

Figure 1 shows the XRD scans of various $MnCl_2$ filling levels for PVDF films. The assigned crystal-

Table I The Assigned Crystalline X-ray Diffraction Peaks

W (wt %)	2θ (Degree)	Assignment
1	20.4	(110) β, (200) β
1	39.6	(002) α
10	21.0	(110) β, (200) β
10	39.8	(002) α
15	20.0	(110) α
15	39.0	(002) α

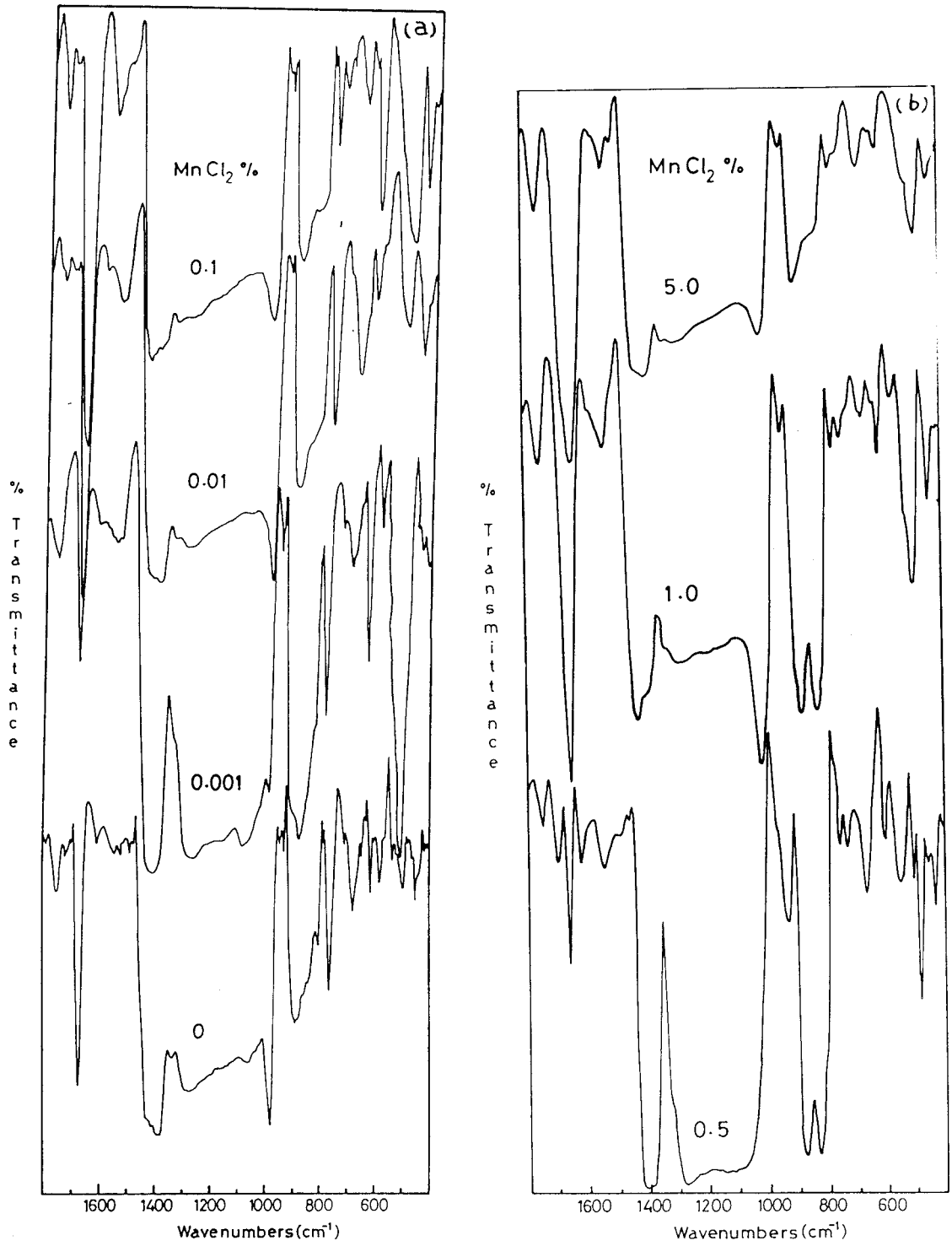

Figure 2 IR transmission spectra for variously filled PVDF films.

line peaks are listed in Table I. These peaks characterize the α- and β-PVDF crystalline[12] phases and the general feature of the observed spectra suggests the presence of a significant fraction of the amorphous PVDF phase. It is clear from Table I that, for 15% filling level, there are no β-phase XRD peaks; and the observed peaks are due only to the α-phase.

IR Analysis

The IR transmission spectra are shown in Figure 2. The main PVDF characterizing frequencies are observed. Furthermore, the IR vibrations due to α-phase[12] (most notably at 490, 530, 618, 796, and 976 cm^{-1}), and the vibrations due to β-phase (at 445, 470, and 510 cm^{-1}) are clearly shown in Figure 2. This confirms the XRD implications about the presence of both α- and β-phases for filling levels $< 15\%$. The structural disorder can be identified by investigation of the filling level dependence of certain IR absorption peaks depicted in Figure 3. The bands at 762 and 990 cm^{-1}, characterizing the α-phase, exhibit changes in their intensity behaviors at 0.1 and 0.5% filling levels. The band at 990 cm^{-1} shows a sharp intensity peak at 1.0% filling level. The band at 1673 cm^{-1}, which is assigned to C=C stretching in the monochlorinated alkenes[13]

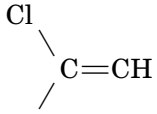

changes its behavior also at 0.1, 0.5, and 1.0% filling levels. It is noteworthy that the C=C mode is a suitable site for polaron formation. The band at 762 cm^{-1} is sensitive to head-to-head (h-to-h) defects. According to the spectroscopic study by Kobayashi et al.,[14] this band corresponds to h-to-h concentration of $\sim$ 12%. This value is comparable with (10%) that obtained by Hasegawa et al. for the pure PVDF.

Optical Absorption

The UV–VIS optical absorption spectra (in the range of 200–800 nm) of the unfilled PVDF and PVDF-filled with various mass fractions of $MnCl_2$ were measured. Figure 4(a–c) depicts the photon energy ($h\nu$) dependence of $\log \alpha$, for the concerned filling levels, where h is plank's constant, ν is the photon frequency, and the absorption coefficient $\alpha(\nu)$ was calculated,[15] using the following formula:

$$\alpha(\nu) = \ln[t_1(\nu)/t_2(\nu)]/(d_2 - d_1) \qquad (1)$$

where t_1 and t_2 are the transmittances of two films (of the same filling level) with thicknesses d_1 and d_2. It is noticed that most of the curves of Figure 4

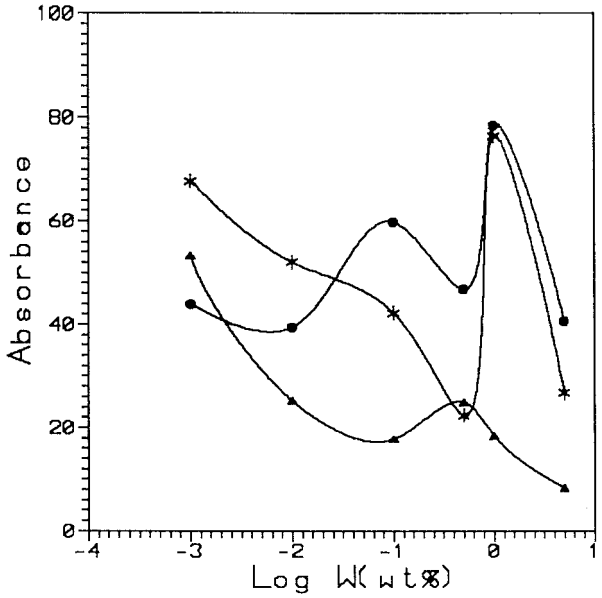

Figure 3 The filling level dependence of some IR absorption peaks at (▲) 762, (∗) 990, and (●) 1673 cm^{-1}.

are characterized by two linear regions, indicating two optical gaps E_{g1} and E_{g2} of values given by[16]

$$\alpha(\nu) = B(h\nu - E_g)^2/h\nu \qquad (2)$$

where B is a constant. The filling level dependences of E_{g1} and E_{g2} are plotted in Figure 5. E_{g1} and E_{g2} experienced minimum values at $W = 0.1$ and 0.5%, respectively. This may arise from the change of the density of the induced energy states due to the change of the $MnCl_2$ filling mode.

DC Electric Conduction

The dc electrical resistivity ρ, was measured in the temperature (T) range of 298–393 K for the present PVDF films. In the present work, the mono- and/or dichlorinated alkenes (detected by the IR analysis), indicating the presence of conjugated polyene, may evidence the formation of polarons and/or bipolarons in the polymeric matrix.[17] Therefore, the present results may be discussed on the basis of the Kuivalainen et al. modified interpolaron hopping model,[18] in which the conduction is attributed to phonon-assisted hopping between polaron and/or bipolaron found states in the polymer. According to this model, the electric resistivity can be expressed as

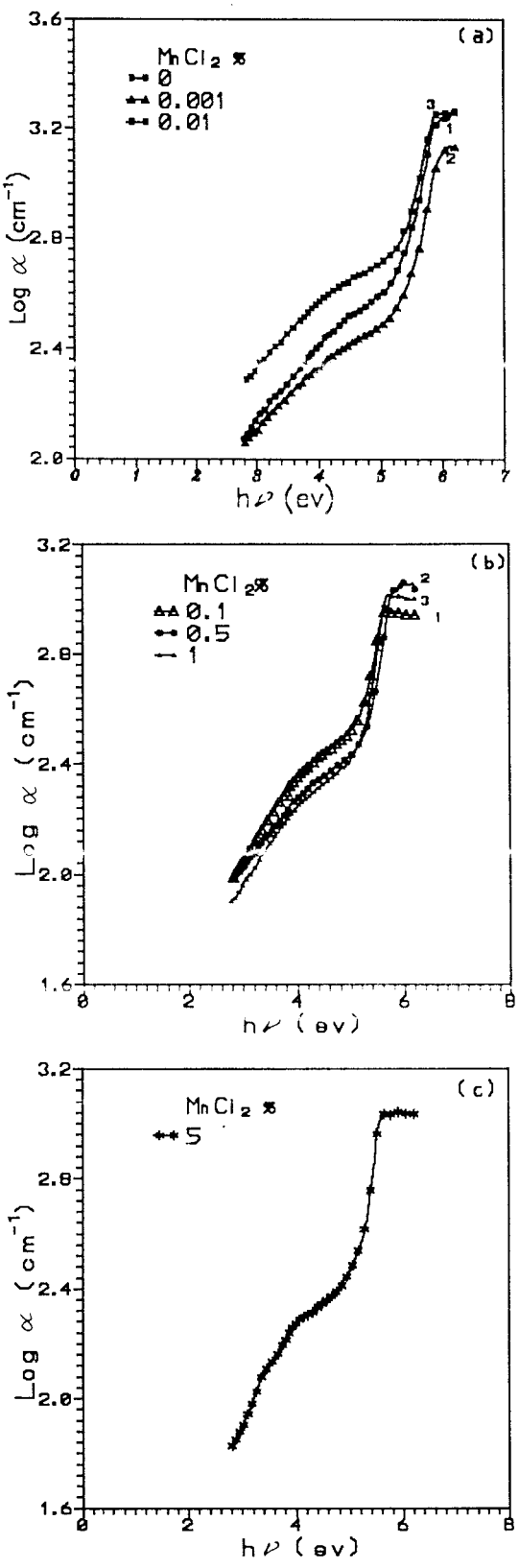

Figure 4 The photon energy ($h\nu$) dependence of log α for variously filled PVDF films.

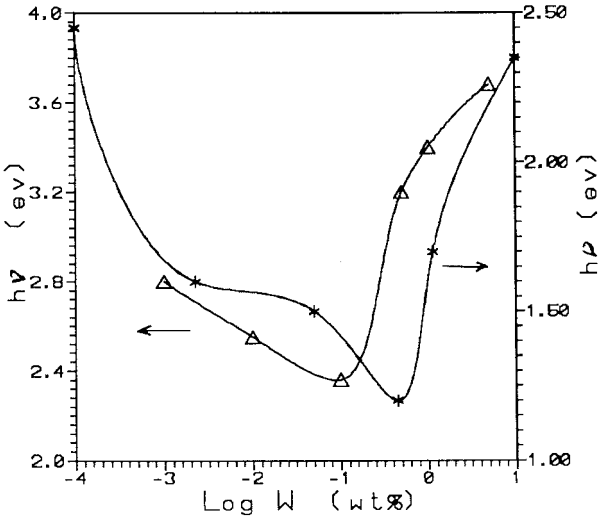

Figure 5 The filling level dependence of E_{g1} and E_{g2} optical gaps.

$$\rho = [kT/A_1e^2\gamma(T)(R_o^2/\zeta)] \times [(Y_p + Y_{bp})^2/(Y_{bp})] \times \exp(2B_1R_o/\zeta) \quad (3)$$

where $A_1 = 0.45$; $B_1 = 1.39$; Y_p and Y_{bp} are the concentration of polaron and bipolaron, respectively; and $R_o = (3/4\pi C_{\text{imp}})^{1/3}$ is the typical separation between impurities whose concentration is C_{imp}; $\xi = (\xi_{11}\xi_\perp)^{1/3}$ is the average decay length of a polaron and bipolaron wave function; and ξ_{11} and $\xi_\perp$ are the decay lengths parallel and perpendicular to the polymer chain, respectively. According to the calculations of Bredas et al.,[19] polarons and bipolarons induce defects of the same extension. The electronic transition rate between polaron and bipolaron states can be expressed as

$$\gamma(T) = \gamma_0(T/300k)^{n+1} \quad (4)$$

where n is a constant ~ 10, and the prefactor, $\gamma_0 = 1.2 \times 10^{17}\ s^{-1}$, was estimated by Kivelson.[20]

The order of magnitude of ρ in the present work was adjusted with the impurity concentration C_{imp}, which actually was the filling parameter. The parameter $\xi_{11} = 1.06$ nm, while $\xi_\perp \approx 0.22$ nm,[21] which depends on the interchain resonance energy and the interchain distance.[22] Taking $Y_p = Y_{bp}$ for simplicity, which is an acceptable approximation,[17] and using eqs. (3) and (4), we can obtain the values of the hopping distance R_o.

The temperature and filling level dependences of R_o are shown in Figure 6, respectively.

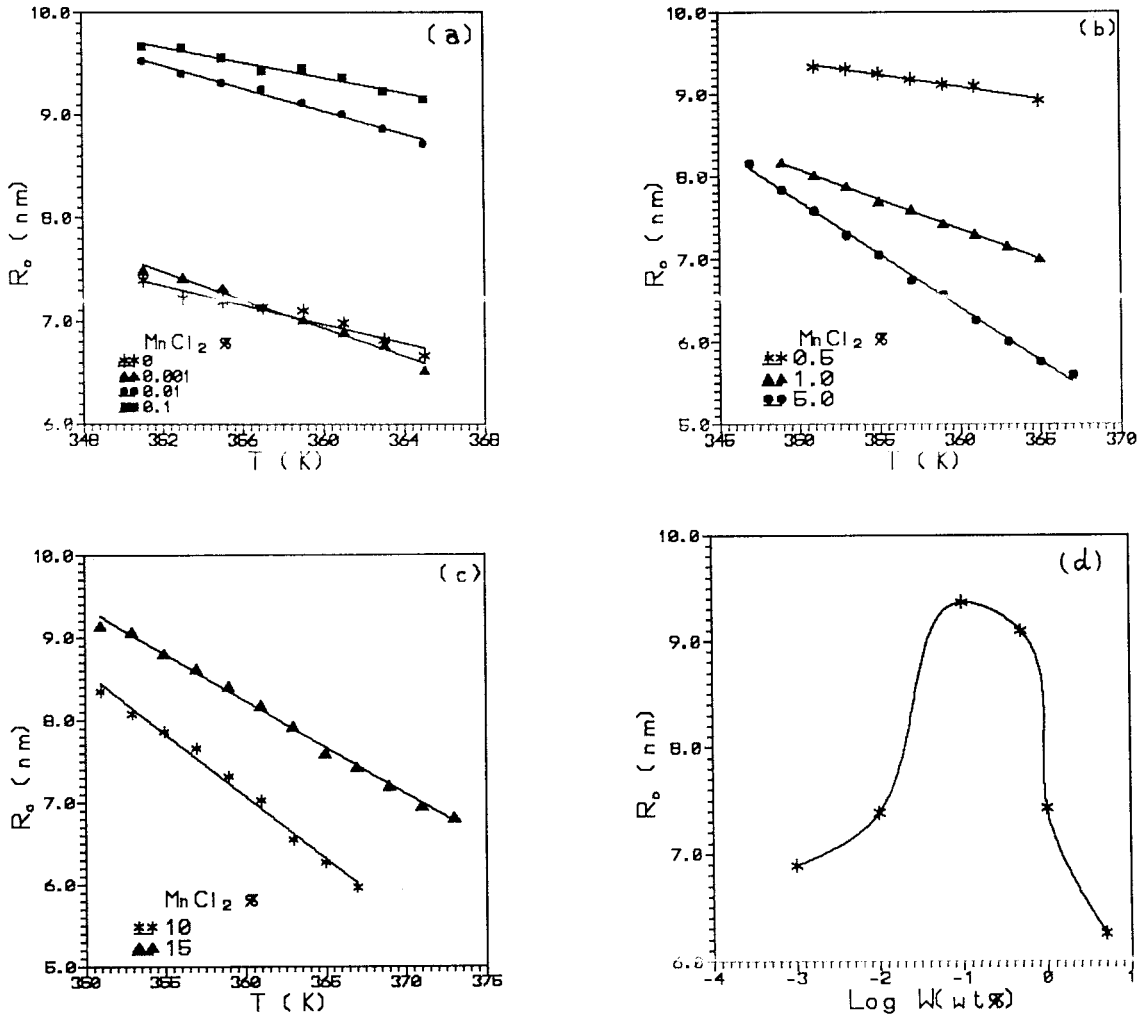

Figure 6 (a–c) The temperature dependence of R_o; (d) the filling level dependence of R_o.

A linear temperature dependence of R_o is noticed, while its filling level dependence exhibits a broad peak around $W \approx 0.1\%$. It is remarkable that the calculated values of R_o are in the range of 6.5–9.7 nm. Considering the monomer unit length to be ≈ 0.25 nm,[23] it can be noticed that the hopping distance is of the range of 26 to 34.4 monomer unit lengths. This indicates that (1) the present conduction mechanism is of an intrachain one-dimensional hopping type; and that (2) the concentration of hopping sites is within the range of 3.9 to 2.9%, which is less than the concentration of h-to-h defect sites ($\sim 12\%$), identified by the IR analysis of the present work (discussed in the preceding IR analysis section). This indicates that the average hopping distance is three or four times the h-to-h defect separation length. Thus, it is thought that not all the defect sites can act as hopping sites. The defect site must exhibit certain local charge and free volume to act as a hopping site. These local charges and free volumes are influenced by $MnCl_2$ filler, which prefers normally to reside in the close vicinity of h-to-h defect.[24]

DC Magnetic Susceptibility

The dc magnetic susceptibility (χ) was measured in the temperature range of 90–270 K, for the present PVDF films. The temperature dependence of the reciprocal susceptibility is plotted in Figure 7. It is clear that χ obeys Curie–Weiss law in which

$$\chi = C/(T + \theta_p) \tag{5}$$

where C is the Curie's constant and θ_p is the paramagnetic Curie temperature. The values of θ_p for various filling levels were calculated using eq. 5, and the values were plotted in Figure 8. Positive θ_p values were found for W up to 10%, indicating the possibility of ferromagnetic interactions between the manganese ions at lower temperatures. On the other hand, the negative θ_p value, obtained for W = 15%, suggests an antiferromagnetic exchange interaction between the manganese ions. A critical filling level (W_c = 14.5%), at which θ_p changes its sign, can be noticed in Figure 8. Moreover, the effective magnetic moment μ_{eff} was calculated, using eq. (6); and the obtained values were plotted as a function of W in Figure 8.

$$\mu_{\text{eff}} = 2.839 \sqrt{\chi_m T} \qquad (6)$$

where χ_m is the molar susceptibility of the filled polymer. It is remarkable that the order of magnitude of μ_{eff} confirms the divalent state of Mn^{2+}.

Electron Spin Resonance

Figure 9 shows ESR spectra of PVDF films of various $MnCl_2$ filling levels. The spectra at low W consisted of six lines and a broad component overlapping the six lines. The six lines are ascribed to the hyperfine structure of the manganese nucleus

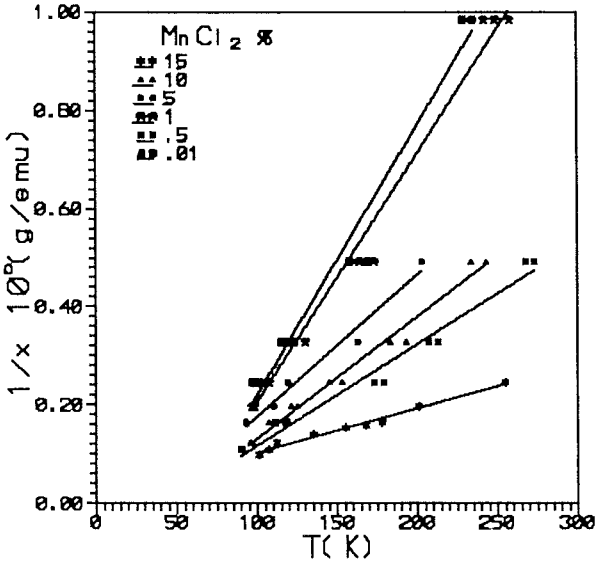

Figure 7 The temperature dependence of the reciprocal magnetic susceptibility for variously filled PVDF films.

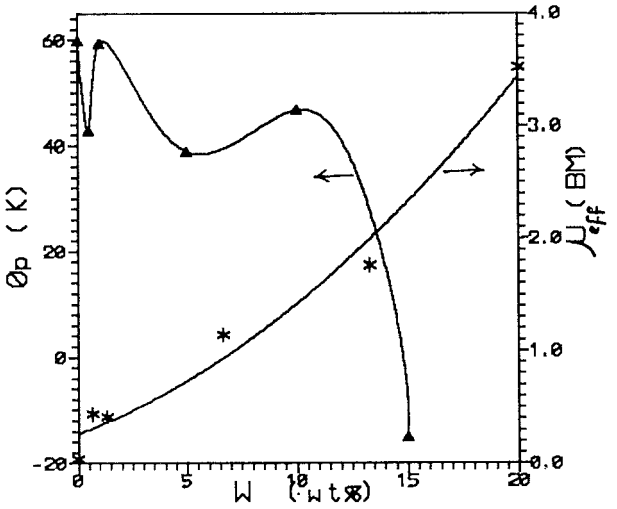

Figure 8 The filling level dependence of θ_p and μ_{eff}.

(I = 5/2) with an unpaired electron, indicating isolated Mn^{2+} in the ionomer. The broad component, of Lorentzian shape, represents the $Mn^{2+} - Mn^{2+}$ exchange interaction, which is caused by the proximity of manganese ions, suggesting[25–27] the presence of aggregated Mn^{2+}. The individual lines of the hyperfine structure became vague with increasing the $MnCl_2$ filling level, indicative of decreasing content of isolated Mn^{2+}. In other words, the increasing content of aggregated Mn^{2+}. Furthermore, the spectrum of PVDF films filled with 25% $MnCl_2$ exhibited a single peak, indicating the absence of isolated Mn^{2+}. The filling level dependence of the filler local structure can be clarified more explicitly with the aid of the peak-to-peak separation (ΔH) of the main ESR Lorentzian signal and the asymmetry factor (A), which is the ratio between the two halves of this signal. The obtained values of ΔH and A are plotted, as functions of W, in Figure 10. It is clear that A decreases as W increases, confirming the implication that Mn^{2+} looses its symmetrical local distribution as the filling level increases. On the other hand, Figure 10 depicts a peak for H around $W \approx 15\%$, supporting the findings of Figure 8 that the $Mn^{2+} - Mn^{2+}$ ferromagnetic exchange interaction transforms to antiferromagnetic one at $W \approx 14.5\%$. It is noteworthy that the magnetic field (H), needed for an antiferromagnetic structure to respond to ESR, is less than that needed for a ferromagnetic one. This explains the decay of ΔH for $W \geq 15\%$.

CONCLUSION

It could be concluded that the present filled PVDF films are characterized by a partially crystalline

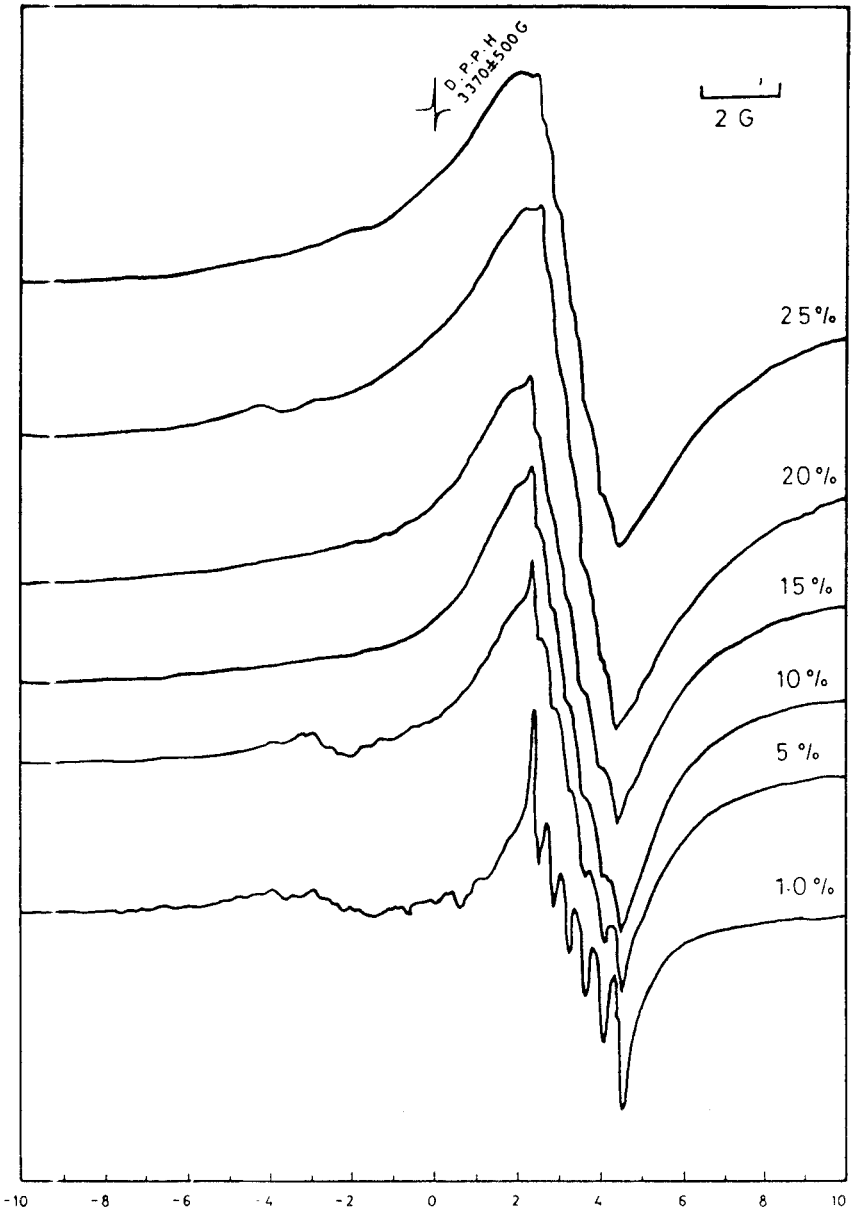

Figure 9 The ESR spectra of PVDF films of various $MnCl_2$ filling levels.

structure with a crystalline part of α- and β-types in the case of $W \leq 10\%$; while for $W = 15\%$ the β-phase disappeared. The IR analysis revealed an h-to-h (and/or t-to-t) concentration of 12%, which is comparable to that found in literature. At 0.1 and 0.5% filling levels, we have noticed the following:

1. The intensity of the IR bands at 762 and 990 cm^{-1} changes its behavior;
2. The two optical gaps E_{g1} and E_{g2} exhibit minimum widths. This was attributed to a change in the $MnCl_2$ filling mode. The dc electrical conduction mechanism was of a one-dimensional intrachain type, based on the phonon-assisted interpolaron hopping model.

The hopping site concentration, calculated according to this model, was within the range of 2.9–3.9% (<12%, the h-to-h concentration). This implied that one-fourth or one-third only of the h-to-h defects may act as a hopping site. The dc magnetic susceptibility exhibited a Cu-

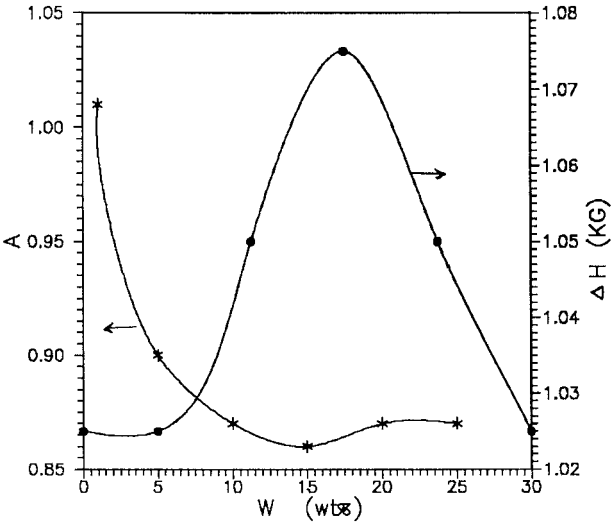

Figure 10 The filling level dependence of ΔH and A.

rie–Weiss temperature dependence, with positive θ_p, indicative of a ferromagnetic exchange interaction between Mn^{2+} ions up to $W = 14.5\%$. Higher W values revealed a negative sign of θ_p due to the antiferromagnetic interactions. The ESR analysis suggested the presence of Mn^{2+} in two different forms, isolated and aggregated. As W increases, the Mn aggregated form predominates.

At $W = 25\%$, the isolated form completely disappears. The present system serves as a good candidate for (1) a one-dimensional electric conduction, (2) sensitive UV–VIS optical absorption, and (2) ferro- or antiferromagnetic interactions. It is remarkable that the above advantages can be added to the well-known other advantages of PVDF, such as the piezo- and pyroelectric effects, as long as the β- or α-phase exists. The α-phase can be easily transformed to polarized phase of high piezo- or pyroelectricity.

REFERENCES

1. T. Hattori, K. Masashi, and O. Hiroji, *J. Appl. Phys.,* **79,** 2016 (1996).
2. P. Bernd, E. Rudolf, and B. Siegfried, *J. Appl. Phys.,* **72,** 5363 (1992).
3. T. Naoto, U. Yoshiaki, and K. Tsuyoshi, *J. Appl. Phys.,* **74,** 3366 (1993).
4. R. Beaulieu, R. A. Lessard, and S. L. Clim, *J. Appl. Phys.,* **79,** 833 (1996).
5. A. Tawansi, H. I. Abdelkader, W. Balachandran, and E. M. Abdelrazek, *J. Mater. Sci.,* **29,** 4001 (1994).
6. B. Servet, S. Ries, and D. Broussoux, *J. Appl. Phys.,* **55,** 2763 (1984).
7. S. Chand and P. C. Mehendru, *J. Phys. D: Appl. Phys.,* **19,** 857 (1986).
8. T. J. Royston, *Noise Control Eng. J.,* **43,** 15 (1995).
9. A. Tawansi, M. I. Ayad, and E. M. Abdelrazek, *J. Mater. Sci. Technol.,* **13,** 124 (1997).
10. A. Tawansi, H. M. Zidan, Y. M. Moustafa, and A. H. Eldumiaty, *Physica Scripta,* **55,** 243 (1997).
11. R. Dingle, M. E. Lines, and S. L. Holt, *Phys. Rev.,* **187,** 643 (1969).
12. G. T. Davis, J. E. McKinney, M. G. Broadhust, and S. C. Roth, *J. Appl. Phys.,* **49,** 4998 (1978).
13. I. Fleming and D. H. Williams, in *Spectroscopic Methods in Organic Chemistry,* McGraw-Hill, New York, 1966, p. 56.
14. M. Kobayashi, K. Tashiro, and H. Tadokoro, *Macromolecules,* **8,** 158 (1975).
15. G. Chiodlli and A. Magistris, *J. Solid State Ionics,* **18–19,** 356 (1986).
16. E. A. Davis and N. F. Mott, *Philos. Mag.,* **22,** 903 (1970).
17. A. Tawansi, H. I. Abdelkader, M. Elzalabany, and E. M. Abdelrazek, *J. Mater. Sci.,* **29,** 3451 (1994).
18. P. Kuivalainen, H. Stubb, H. Isotlo, P. Yli, and C. Holmstrom, **B31, 7900** (1985).
19. J. L. Bredas, R. R. Chance, and R. Silbeyey, *Phys. Rev.,* **B26,** 5843 (1982).
20. S. Kivelson, *Phys. Rev.,* **B25,** 3798 (1982).
21. N. F. Mott and R. W. Gurrey, in *Electronic Processes in Ionic Crystals,* Oxford University Press, London, 1940, p. 34.
22. S. Kivelson, *Phys. Rev. Lett.,* **46,** 1344 (1981).
23. R. Hazegawa, Y. Takahasli, Y. Chatwi, and H. Tadakoro, *Polym. J.,* **3,** 600 (1972).
24. D. K. Das-Gupta, K. Doughty, and R. S. Brockley, *J. Phys. D: Appl. Phys.,* **13,** 2101 (1980).
25. S. Yano, H. Yamashita, M. Matsushita, K. Aoki, and J. Yamauchi, *Colloid Polym. Sci.,* **259,** 514 (1981).
26. I. Yamauchi and S. Yano, *Macromolecules,* **15,** 210 (1982).
27. H. Toriumi, R. A. Weiss, and H. A. Frank, *Macromolecules,* **17,** 2104 (1984).